Effects of semiconduction on electromechanical energy conversion in piezoelectrics

2015 Smart Mater. Struct. 24 025021

(http://iopscience.iop.org/0964-1726/24/2/025021)

IOP Publishing Smart Materials and Structures
Smart Mater. Struct. **24** (2015) 025021 (7pp) doi:10.1088/0964-1726/24/2/025021

Effects of semiconduction on electromechanical energy conversion in piezoelectrics

Peng Li[1], **Feng Jin**[2] **and Jiashi Yang**[3]

[1] School of Human Settlements and Civil Engineering, Xi'an Jiaotong University, Xi'an, Shaanxi 710049, People's Republic of China

[2] State Key Laboratory for Strength and Vibration of Mechanical Structures, Xi'an Jiaotong University, Xi'an, Shaanxi 710049, People's Republic of China

[3] Department of Mechanical and Materials Engineering, University of Nebraska-Lincoln, Lincoln, NE 68588-0526, USA

E-mail: jinfengzhao@263.net

Received 14 July 2014, revised 6 November 2014
Accepted for publication 4 December 2014
Published 8 January 2015

Abstract

We study the effect of semiconduction on mechanical-to-electrical energy conversion through a theoretical analysis on the thickness-extensional vibration of a piezoelectric semiconductor plate driven mechanically. An analytical solution is obtained. A ZnO plate is used as a numerical example. Results show that both the electrical output power and the energy conversion efficiency are sensitive to semiconduction at a moderate carrier density of 10^{15} m^{-3}, and that the effect of the dissipation due to semiconduction can be comparable to the effect of material damping when the material quality factor is in the usual range of 10^2–10^3.

Keywords: piezoelectric semiconductors, thickness-extensional vibration, output electrical power, energy conversion efficiency

(Some figures may appear in colour only in the online journal)

1. Introduction

Piezoelectric materials are widely used to make electromechanical transducers for converting electric energy to mechanical energy or vice versa. Relatively recently, because of the rapid development of wireless electronic devices, operating these devices without a wired power source has become an important issue. One approach is to harvest power from the operating environment. Piezoelectric materials are natural candidates for devices that scavenge ambient power by converting mechanical energy into electric energy for powering small electronic devices with a low power requirement. Such a piezoelectric device is called a piezoelectric generator or energy harvester. Piezoelectric energy harvesters have received broad and sustained attention [1, 2].

Piezoelectric materials are usually used and treated as dielectrics (insulators) without electrical conduction. In fact, there is no sharp line separating conductors from insulators. Real materials more or less have some electrical conduction [3]. For example, in acoustic wave devices made from quartz piezoelectric crystals which are usually considered as good insulators, the small Ohmic conduction and the related dissipative effects need to be considered when calculating the Q value (quality factor) of the devices [4–6] because the other dissipative effects in quartz such as material damping are also very small.

Another origin of conduction in piezoelectric materials is that some of them are semiconductors [7], e.g., the widely used ZnO and AlN films and fibers. In these materials, in addition to carrier drift under an electric field which is associated with Ohmic conduction, carrier diffusion also contributes to the current. Piezoelectric semiconductors have been used to make devices for acoustic wave amplification [8–11] and acoustic charge transport [12, 13] based on the acoustoelectric effect, i.e., the motion of carriers under the electric field accompanying an acoustic wave. Recently, piezoelectric semiconductors such as ZnO are also used for mechanical energy harvesting and conversion to electric

energy [14–17]. Taking ZnO nanowires for example, they have been applied in energy harvester [18–21], which address the potential for nanoscale energy harvesting.

At present there is little understanding of the effects of conduction/semiconduction on energy conversion in piezoelectric materials. In this paper we examine these effects by studying the thickness-extensional vibration of a piezoelectric semiconductor plate driven by mechanical loads with an electrical output. Conductions of Ohmic and diffusive origins are both considered. A theoretical analysis is performed using the linear theory of acoustoelectricity.

2. Governing equations

The basic behavior of piezoelectric semiconductors can be described by a linear phenomenological theory [8, 22]. Consider a one-carrier piezoelectric semiconductor whose carrier charge and steady state carrier density are q and $\bar{n}$, respectively. When an acoustic wave propagates through the material, it produces an electric field E_j and an electric current J_i. The perturbation of the carrier density is denoted by n. The linear theory for small and dynamic signals in a piezoelectric semiconductor consists of the equations of motion (Newton's law), Gauss's law of electrostatics, and the conservation of charge:

$$\begin{aligned} &T_{ji,j} = \rho \ddot{u}_i, \\ &D_{i,i} = qn, \\ &q\dot{n} + J_{i,i} = 0, \end{aligned} \tag{1}$$

where u_i is the displacement vector, T_{ij} is the stress tensor, ρ is the mass density, and D_i is the electric displacement vector. The Cartesian tensor notation and the summation convention for repeated indices are employed. A comma followed by an index denotes partial differentiation with respect to the coordinate associated with the index. A superimposed dot represents differentiation with respect to time t. The above equations are accompanied by the following constitutive relations:

$$\begin{aligned} T_{ij} &= c_{ijkl}S_{kl} - e_{kij}E_k, \\ D_i &= e_{ijk}S_{jk} + \varepsilon_{ij}E_j, \\ J_i &= q\bar{n}\mu_{ij}E_j - qd_{ij}n_{,j}, \end{aligned} \tag{2}$$

where the strain tensor S_{ij} and the electric field E_k are related to the displacement u_i and the electric potential ϕ by

$$\begin{aligned} S_{ij} &= \left(u_{i,j} + u_{j,i}\right)/2, \\ E_i &= -\phi_{,i}. \end{aligned} \tag{3}$$

In (2), c_{ijkl}, e_{kij} and ε_{ij} are the elastic, piezoelectric and dielectric constants. μ_{ij} and d_{ij} are the carrier mobility and diffusion constants. With successive substitutions from (2) and (3), we can write (1) as five equations for u_i, ϕ and n:

$$\begin{aligned} &c_{ijkl}u_{k,lj} + e_{kij}\phi_{,kj} = \rho \ddot{u}_i, \\ &e_{ikl}u_{k,li} - \varepsilon_{ij}\phi_{,ij} = qn, \\ &\dot{n} - \bar{n}\mu_{ij}\phi_{,ij} - d_{ij}n_{,ij} = 0. \end{aligned} \tag{4}$$

On the boundary of a finite body, the mechanical displacement u_i or the traction vector, the electric potential ϕ or the normal component of the electric displacement vector, the carrier density n or the normal current, or the combinations of some of them may be prescribed [3].

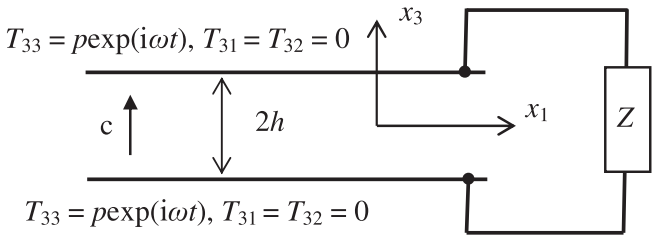

Figure 1. A piezoelectric semiconductor plate and coordinate system.

3. Thickness-extensional motion of a plate

Consider an unbounded piezoelectric semiconductor plate of crystals of class 6 mm with the c axis along x_3 as shown in figure 1. This includes widely used materials such as ZnO and AlN. The two surfaces of the plate are driven by a time-harmonic surface normal stress p. The plate surfaces are electroded. We consider the relatively simple case of Ohmic or non-rectifying contact between the plate and the electrodes. The electrodes are joined by an output circuit whose impedance is Z in harmonic motions. The plate is driven into pure thickness-extensional motion [23] by the surface stress with one displacement component $u_3 = u(x_3, t)$ along with $\phi = \phi(x_3, t)$ and $n = n(x_3, t)$. We denote the relevant elastic, piezoelectric and dielectric constants by $c_{33} = c$, $e_{33} = e$, and $\varepsilon_{33} = \varepsilon$. Similarly, the relevant mobility and diffusion coefficient are denoted by $\mu_{33} = \mu$ and $d_{33} = d$. Then (4) takes the following form:

$$\begin{aligned} &cu_{,33} + e\phi_{,33} = \rho \ddot{u}, \\ &eu_{,33} - \varepsilon\phi_{,33} = qn, \\ &\dot{n} - \bar{n}\mu\phi_{,33} - dn_{,33} = 0. \end{aligned} \tag{5}$$

We also denote $T_{33} = T$, $S_{33} = S$, $D_3 = D$, and $J_3 = J$. The mechanical boundary conditions at the plate surfaces where $x_3 = \pm h$ are

$$T = p\exp(i\omega t). \tag{6}$$

The free charge per unit area Q_3 on the electrode at $x_3 = h$ is given by

$$Q_3 = -D. \tag{7}$$

The current per unit area that flows out of the electrode at $x_3 = h$ is

$$I = J - \dot{Q}_3. \tag{8}$$

We denote the potential difference between the two electrodes by a voltage V through

$$\phi(x_3 = h) - \phi(x_3 = -h) = V. \tag{9}$$

For time-harmonic motions, we use the usual complex notation. For example,

$$\{V, Q_3, I, J\} = \mathrm{Re}\left\{\left(\bar{V}, \bar{Q}_3, \bar{I}, \bar{J}\right)\exp(\mathrm{i}\omega t)\right\}. \tag{10}$$

The common time-harmonic factor will be neglected. We have the following relation for the output circuit:

$$\bar{I} = \bar{V}/Z. \tag{11}$$

When Z is infinite, we effectively have an open circuit. When $Z = 0$, the electrodes are shorted. Note that in general Z may be a function of ω, which depends on the structure of the output circuit. (6) and (11) are similar to the two corresponding boundary conditions in [23] for a piezoelectric dielectric plate. Since we are considerating a semiconductor plate with one more field n and one more equation $(5)_3$, we need another boundary condition which we take to be the prescription of the carrier density perturbation near the boundary:

$$n = n_0, \tag{12}$$

which is experimentally measurable.

4. Analytical solution for time-harmonic thickness-extensional vibration

We look for a solution in the following form:

$$\begin{cases} u &= A\mathrm{e}^{\xi x_3}\exp(\mathrm{i}\omega t), \\ \phi &= B\mathrm{e}^{\xi x_3}\exp(\mathrm{i}\omega t), \\ n &= C\mathrm{e}^{\xi x_3}\exp(\mathrm{i}\omega t), \end{cases} \tag{13}$$

where A, B, C and ξ are undetermined constants. The substitution of (13) into (5) leads to a system of homogeneous linear equations for A, B and C:

$$\begin{cases} \left(c\xi^2 + \rho\omega^2\right)A + e\xi^2 B = 0, \\ e\xi^2 A - \varepsilon\xi^2 B - qC = 0, \\ \bar{n}\mu\xi^2 B + \left(d\xi^2 - \mathrm{i}\omega\right)C = 0. \end{cases} \tag{14}$$

The common exponential factor will be dropped in the following. For nontrivial solutions of A, B or C, the determinant of the coefficient matrix of (14) has to vanish. This yields the following algebraic equation for ξ:

$$\left[\left(c\xi^2 + \rho\omega^2\right)\frac{q\bar{n}\mu}{\varepsilon} - \left(\bar{c}\xi^2 + \rho\omega^2\right)\left(d\xi^2 - \mathrm{i}\omega\right)\right]\xi^2 = 0. \tag{15}$$

(15) has six roots:

$$\begin{aligned} &\xi_{1,2} = 0, \\ &\xi_{3,4} = \pm\sqrt{\frac{-B' + \sqrt{B'^2 - 4A'C'}}{2A'}}, \\ &\xi_{5,6} = \pm\sqrt{\frac{-B' - \sqrt{B'^2 - 4A'C'}}{2A'}}, \end{aligned} \tag{16}$$

where

$$\begin{aligned} A' &= -\bar{c}d, \\ B' &= \frac{cq\bar{n}\mu}{\varepsilon} - \rho\omega^2 d + \mathrm{i}\omega\bar{c}, \\ C' &= \rho\omega^2\left(\frac{q\bar{n}\mu}{\varepsilon} + \mathrm{i}\omega\right). \end{aligned} \tag{17}$$

Because of the symmetry in the problem, only three of the above six roots are needed to construct a solution with the necessary symmetry. We denote

$$\begin{aligned} &\lambda_1 = \xi_1 = 0, \\ &\lambda_2 = \xi_3 = \sqrt{\frac{-B' + \sqrt{B'^2 - 4A'C'}}{2A'}}, \\ &\lambda_3 = \xi_5 = \sqrt{\frac{-B' - \sqrt{B'^2 - 4A'C'}}{2A'}}. \end{aligned} \tag{18}$$

Then the displacement, electric potential and carrier density perturbation can be written as

$$\begin{cases} u &= \alpha_2 A_2\sinh(\lambda_2 x_3) + \alpha_3 A_3\sinh(\lambda_3 x_3), \\ \phi &= A_1 x_3 + A_2\sinh(\lambda_2 x_3) + A_3\sinh(\lambda_3 x_3), \\ n &= \beta_2 A_2\sinh(\lambda_2 x_3) + \beta_3 A_3\sinh(\lambda_3 x_3), \end{cases} \tag{19}$$

where A_1, A_2 and A_3 are undetermined constants and

$$\alpha_m = \frac{-e\lambda_m^2}{c\lambda_m^2 + \rho\omega^2},\quad \beta_m = \frac{\bar{n}\mu\lambda_m^2}{\mathrm{i}\omega - d\lambda_m^2},\quad (m = 2,3). \tag{20}$$

With (19), the stress, electric displacement and current components needed for the boundary conditions can be expressed as

$$\begin{cases} T &= (c\alpha_2 + e)\lambda_2 A_2\cosh(\lambda_2 x_3) \\ &\quad + (c\alpha_3 + e)\lambda_3 A_3\cosh(\lambda_3 x_3) + eA_1, \\ D &= (e\alpha_2 - \varepsilon)\lambda_2 A_2\cosh(\lambda_2 x_3) \\ &\quad + (e\alpha_3 - \varepsilon)\lambda_3 A_3\cosh(\lambda_3 x_3) - \varepsilon A_1, \\ J &= -q\left(\bar{n}\mu + d\beta_2\right)\lambda_2 A_2\cosh(\lambda_2 x_3) \\ &\quad - q\left(\bar{n}\mu + d\beta_3\right)\lambda_3 A_3\cosh(\lambda_3 x_3) - q\bar{n}\mu A_1. \end{cases} \tag{21}$$

With the symmetry in the problem, we only need to consider the boundary conditions at $x_3 = h$. Substituting (19) and (21) into (6), (11) and (12), we obtain the following three linear

equations for A_1, A_2 and A_3:

$$\begin{aligned}
&(c\alpha_2 + e)\lambda_2 A_2 \cosh(\lambda_2 h) + (c\alpha_3 + e) \\
&\quad \times \lambda_3 A_3 \cosh(\lambda_3 h) + eA_1 = p, \\
&\beta_2 A_2 \sinh(\lambda_2 h) + \beta_2 A_2 \sinh(\lambda_2 h) = n_0, \\
&\quad -\left[(\mathrm{i}\omega\varepsilon + q\bar{n}\mu)Z + 2h\right]A_1 \\
&\quad + \left\{\left[\mathrm{i}\omega(e\alpha_2 - \varepsilon) - q\left(\bar{n}\mu + d\beta_2\right)\right]\right. \\
&\quad \times \lambda_2 Z\cosh(\lambda_2 h) - \left.2\sinh(\lambda_2 h)\right\}A_2 \\
&\quad + \left\{\left[\mathrm{i}\omega(e\alpha_3 - \varepsilon) - q\left(\bar{n}\mu + d\beta_3\right)\right]\right. \\
&\quad \times \lambda_3 Z\cosh(\lambda_3 h) - \left.2\sinh(\lambda_3 h)\right\}A_3 = 0.
\end{aligned} \tag{22}$$

The solution of (22) for A_1, A_2 and A_3 is given by

$$\begin{aligned}
A_2 &= \frac{p(1 + Z/Z_0)\beta_3 \sinh(\lambda_3 h) - en_0 N}{e\left[M\beta_3 \sinh(\lambda_3 h) - N\beta_2 \sinh(\lambda_2 h)\right]}, \\
A_3 &= \frac{-p(1 + Z/Z_0)\beta_2 \sinh(\lambda_2 h) + en_0 M}{e\left[M\beta_3 \sinh(\lambda_3 h) - N\beta_2 \sinh(\lambda_2 h)\right]}, \\
A_1 &= \frac{p}{e} - \left(\frac{c}{e}\alpha_2 + 1\right)\lambda_2 \cosh(\lambda_2 h)A_2 \\
&\quad - \left(\frac{c}{e}\alpha_3 + 1\right)\lambda_3 \cosh(\lambda_3 h)A_3,
\end{aligned} \tag{23}$$

where

$$\begin{aligned}
M &= \frac{\mathrm{i}\omega(e\alpha_2 - \varepsilon) - q\left(\bar{n}\mu + d\beta_2\right)}{\mathrm{i}\omega\varepsilon + q\bar{n}\mu} \\
&\quad \times \lambda_2 \frac{Z}{Z_0}\cosh(\lambda_2 h) \\
&\quad - \frac{\sinh(\lambda_2 h)}{h} + \left(\frac{c}{e}\alpha_2 + 1\right)\left(1 + \frac{Z}{Z_0}\right) \\
&\quad \times \lambda_2 \cosh(\lambda_2 h), \\
N &= \frac{\mathrm{i}\omega(e\alpha_3 - \varepsilon) - q\left(\bar{n}\mu + d\beta_3\right)}{\mathrm{i}\omega\varepsilon + q\bar{n}\mu} \\
&\quad \times \lambda_3 \frac{Z}{Z_0}\cosh(\lambda_3 h) \\
&\quad - \frac{\sinh(\lambda_3 h)}{h} + \left(\frac{c}{e}\alpha_3 + 1\right)\left(1 + \frac{Z}{Z_0}\right) \\
&\quad \times \lambda_3 \cosh(\lambda_3 h), \\
Z_0 &= \frac{2h}{\mathrm{i}\omega\varepsilon + q\bar{n}\mu}.
\end{aligned} \tag{24}$$

The average input mechanical power per unit plate area during a period is given by [23]

$$P_1 = 2\left[\frac{1}{4}\left(pv_3^* + p^* v_3\right)\right], \tag{25}$$

where v_3 is the thickness-extensional velocity component and an asterisk represents complex conjugate. The average output electrical power per unit plate area can be calculated from [23]

$$\begin{aligned}
P_2 &= \frac{1}{4}\left(\bar{I}\bar{V}^* + \bar{I}^*\bar{V}\right) \\
&= \frac{1}{4}\bar{I}\ \bar{I}^*(Z + Z^*) \\
&= \frac{1}{2}\left|\bar{I}\right|^2 \mathrm{Re}\{Z\}.
\end{aligned} \tag{26}$$

Then the efficiency of the conversion of the input mechanical power into the output electric power is [23]

$$\eta = \frac{P_2}{P_1}. \tag{27}$$

5. Numerical results and discussion

For numerical results we consider a plate of ZnO with [24] $c = 211$ GPa, $e = 1.32\ \mathrm{C\,m^{-2}}$, $\varepsilon = 8.85 \times 10^{-11}\ \mathrm{F\,m^{-1}}$, $\rho = 5700\ \mathrm{kg\,m^{-3}}$, $q = 1.602 \times 10^{-19}$ C, $\mu = 1350\ \mathrm{cm^2\,V^{-1}\,s^{-1}}$ and $d = \mu kT/q$ [25]. k is the Boltzmann constant and T is the absolute temperature. $T = 300\ ^\circ$K is used. The mechanical damping of the material is introduced through replacing the relevant elastic constant c by a complex number $c(1 + \mathrm{i}Q^{-1})$ where Q is a real, positive and large number. It can describe viscoelastic behaviors of the material. To focus on the dissipation due to semiconduction, we must leave the effect of material damping out, i.e., Q is set to infinity, in figures 2–6. For the surface mechanical load, $p = 1\ \mathrm{N\,m^{-2}}$ is used in our calculation. We only consider surface mechanical load and set $n_0 = 0$. The plate thickness is $2h = 2$ cm except in figure 5. The steady state carrier density $\bar{n}$ can range from zero to $10^{19}\ \mathrm{m^{-3}}$. The load impedance of the output circuit is taken to be $Z = (1 + \mathrm{i})Z_0$ except in figure 6. We introduce the following frequency to normalize the driving frequency:

$$\omega_s = \frac{\pi}{2h}\sqrt{\frac{\bar{c}}{\rho}}, \tag{28}$$

which is the fundamental thickness-extensional frequency of the plate and is equal to $\omega_s = 9.993 \times 10^5\ \mathrm{rad\,s^{-1}}$ when $h = 1$ cm.

Figure 2 shows the basic behavior of the energy conversion in the plate, i.e., the output power P_2 versus the driving frequency ω. Only symmetric modes of thickness-extensional motion are considered, such as equation (19), the displacement, electric potential and carrier density perturbation are all odd functions about mid-plane of the plate $x_3 = 0$. No anti-symmetric modes of thickness-extensional motion are included. Therefore, the output is significant only at a series of discrete frequencies which are the odd thickness-extensional resonant frequencies of the plate. They are close to 1, 3, and 5, … when normalized by ω_s. The difference between figures 2(a) and (b) is that in (a) the steady state carrier density $\bar{n} = 0$ and there is no dissipation due to conduction, while in (b) there is a moderate $\bar{n} = 10^{14}\ \mathrm{m^{-3}}$. Because of the resistive component in Z, the resonances are not singular even when $\bar{n} = 0$. Sufficient data points are used to capture the

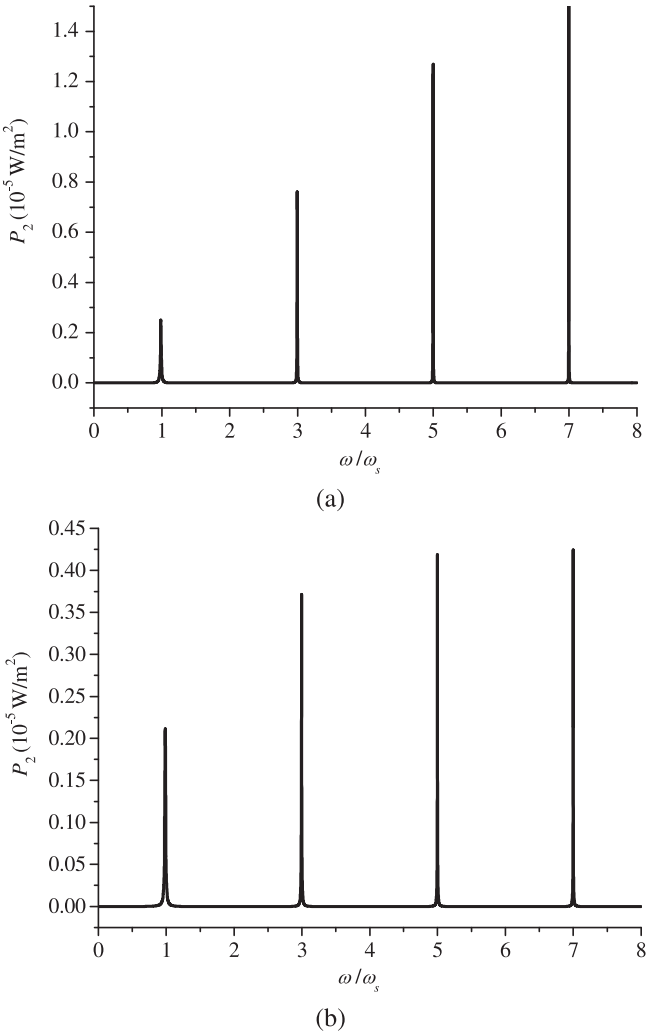

Figure 2. Output electrical power per unit plate area versus driving frequency with $h = 1$ cm, $Q = \infty$ and $Z = (1 + \mathrm{i})Z_0$: (a) $\bar{n} = 0$; and (b) $\bar{n} = 1 \times 10^{14}$ m^{-3}.

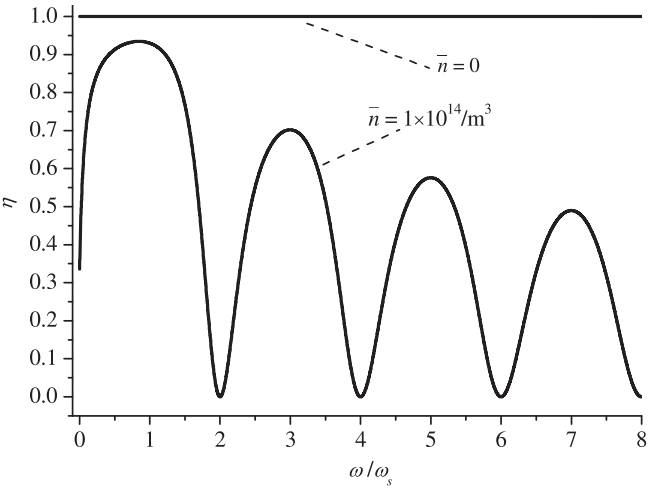

Figure 3. Efficiency versus driving frequency with $h = 1$ cm, $Q = \infty$, and $Z = (1 + \mathrm{i})Z_0$.

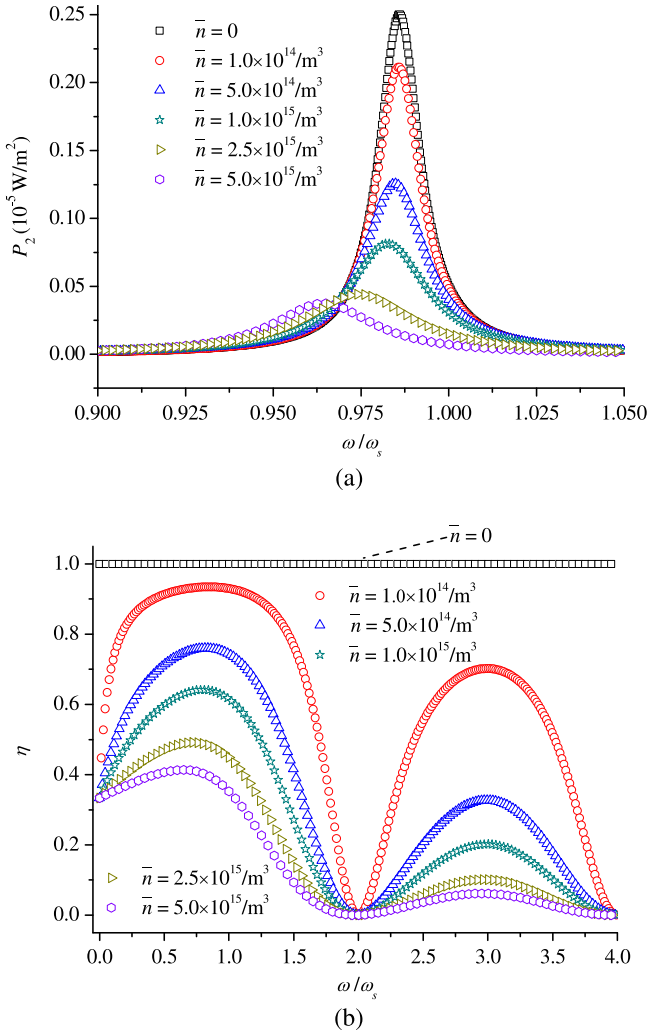

Figure 4. Effect of $\bar{n}$ with $h = 1$ cm, $Q = \infty$, and $Z = (1 + \mathrm{i})Z_0$: (a) P_2 near the first resonance; and (b) efficiency at the first two resonances.

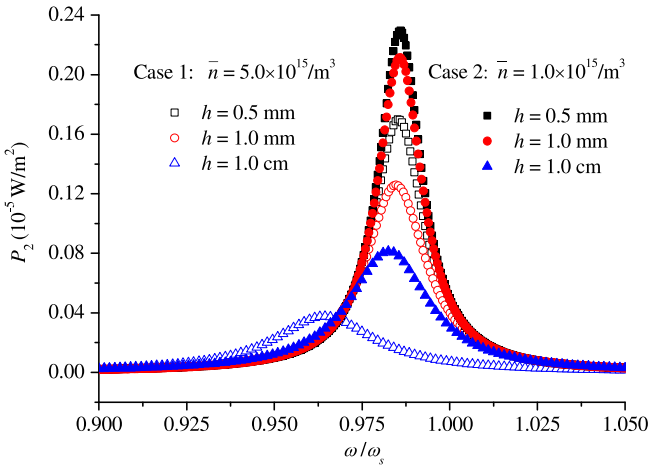

Figure 5. Effect of the plate thickness $2h$ and $\bar{n}$ on P_2 near the first resonance with $Q = \infty$, and $Z = (1 + \mathrm{i})Z_0$.

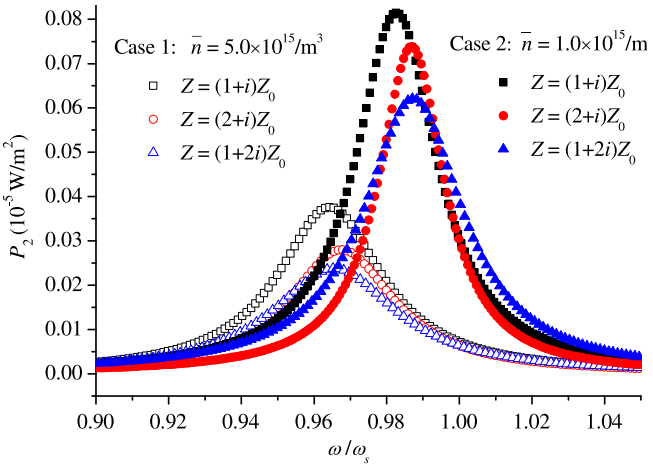

Figure 6. Effect of the load impedance Z and $\bar{n}$ on P_2 near the first resonance with $h = 1$ cm, and $Q = \infty$.

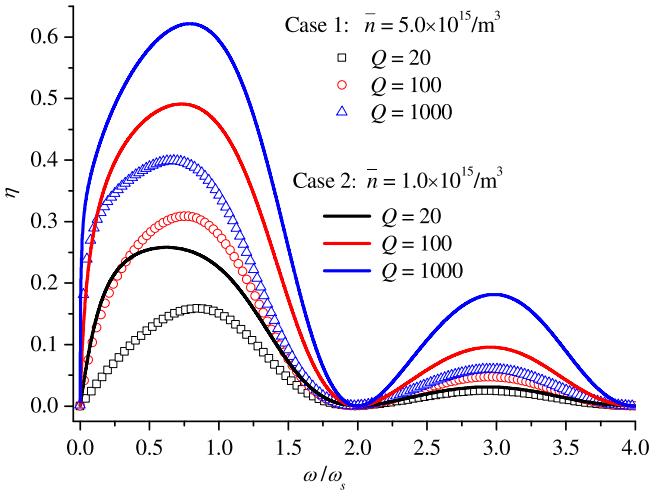

Figure 7. Effect of material mechanical damping Q on efficiency with $h = 1$ cm, and $Z = (1 + i)Z_0$.

maxima accurately. Compared to (a), P_2 is significantly lowered in (b) by $\bar{n}$ and the related semiconduction as expected.

Figure 3 shows the basic behavior of efficiency versus driving frequency at the first few resonances for the same two values of $\bar{n} = 0$ and $\bar{n} = 1 \times 10^{14}$ m^{-3} as those used in figure 2. When $\bar{n} = 0$, there is no energy loss in the plate and the efficiency is identically equal to one. However, for a moderate $\bar{n} = 1 \times 10^{14}$ m^{-3} and the related dissipation in the plate due to semiconduction, the efficiency drops significantly. The efficiency is still relatively high near resonances. At the first resonance it is as high as 90%. This is not surprising piezoelectric generators [23].

For a closer look at the effect of the steady state carrier density $\bar{n}$ on the output power P_2, in figure 4(a) we plot P_2 near the first resonance for a series of values of $\bar{n}$. Clearly, once $\bar{n}$ reaches the level of 10^{14} m^{-3} or higher, P_2 becomes very sensitive to $\bar{n}$. A larger $\bar{n}$ implies more dissipation due to semiconduction and a weaker resonance as expected. In figure 4(b) the efficiency at the first two resonances are shown for multiple values of $\bar{n}$. It can be seen that the efficiency of the energy conversion is also sensitive to $\bar{n}$ and is significantly lowered once $\bar{n}$ reaches 10^{14} m^{-3} and above. From perspective of physics, it has been revealed that a too high carrier density would screen the piezoelectric charges, thus resulting in a lower or even vanishing output current [26, 27]. Hence, the output power P_2 has been reduced evidently, which indicates that the increasing of carrier density is not beneficial for improving the output power [26].

Figure 5 shows the output power P_2 at the first resonance for different plate thickness $2h$ and two values of $\bar{n}$. For each plate thickness, the corresponding ω_s is used so that the normalized resonant frequency is always close to 1. For the same plate thickness, there are two curves for different $\bar{n}$. The difference between the two curves varies as the plate thickness changes. At the high frequency end with a small h, the electric field in the plate reverses its directions very quickly which makes it difficult for semiconduction to happen significantly. Therefore the peaks are higher for smaller values of h and the difference between the too curves with the same h also become smaller at the high frequency end with a small h.

Figure 6 shows the effect of the load impedance Z and $\bar{n}$ on P_2 near the first resonance. P_2 is sensitive to both, showing that in this case the dissipation due to semiconduction is comparable to the output power.

Figure 7 is the only figure in which the effect of the material mechanical damping described by Q is included. For the values of Q and $\bar{n}$ shown, the efficiency is about equally sensitive to both. A smaller Q or a larger $\bar{n}$ means more dissipation due to either material damping or semiconduction and hence a lower efficiency as expected.

6. Conclusion

The output electrical power and the energy conversion efficiency assume maxima at or near the plate thickness-extensional resonant frequencies. The efficiency can be very high as also seen from [23]. The output power and the efficiency are both sensitive to the semiconduction. Specifically, for a ZnO plate with mm thickness and MHz resonant frequencies, when the initial carrier density is moderate and is of the order of 10^{15} m^{-3}, the dissipative effect due to semiconduction is significant and comparable to the effect of material mechanical damping when the material quality factor Q varies from 20 to 1000.

Acknowledgments

The National Natural Science Foundation of China (Nos. 11272247 and 11402187), China Postdoctoral Science Foundation funded project (2014M560762) and the National 111 Project of China (No. B06024) are gratefully acknowledged for their financial support.

References

[1] Sodano H A and Inman D J 2007 A review of power harvesting from vibration using piezoelectric materials (2003–2006) *Smart Mater. Struct.* **16** R1–21

[2] Twiefel J and Westermann H 2013 Survey on broadband techniques for vibration energy harvesting *J. Intell. Mater. Syst. Struct.* **24** 1291–302

[3] Tiersten H F and Sham T L 1998 On the necessity of including electrical conductivity in the description of piezoelectric fracture in real materials *IEEE Trans. Ultrason. Ferroelectr. Freq. Control* **45** 1–3

[4] Yong Y K, Patel M S and Tanaka M 2010 Theory and experimental verifications of the resonator *Q* and equivalent electrical parameters due to viscoelastic and mounting supports losses *IEEE Trans. Ultrason. Ferroelectr. Freq. Control* **57** 1831–9

[5] Lee P C Y, Liu N H and Ballato A 2004 Thickness vibrations of a piezoelectric plate with dissipation *IEEE Trans. Ultrason. Ferroelectr. Freq. Control* **51** 52–62

[6] Wang J, Zhao W H, Du J K and Hu Y T 2011 The calculation of electrical parameters of AT-cut quartz crystal resonators with the consideration of material viscosity *Ultrasonics* **51** 65–70

[7] Auld B A 1973 *Acoustic Fields and Waves in Solids* vol 1 (New York: Wiley)

[8] White D L 1962 Amplification of ultrasonic waves in piezoelectric semiconductors *J. Appl. Phys.* **33** 2547–54

[9] Yang J S and Zhou H G 2004 Acoustoelectric amplification of piezoelectric surface waves *Acta Mech.* **172** 113–22

[10] Ghosh S and Khare P 2006 Acoustic wave amplification in ion-implanted piezoelectric semiconductor *Indian J. Pure Appl. Phys.* **44** 183–7

[11] Willatzen M and Christensen J 2014 Acoustic gain in piezoelectric semiconductors at epsilon-near-zero response *Phys. Rev.* B **89** 041201

[12] Schulein F J R, Muller K, Bichler M, Koblmuller G, Finley J J, Wixforth A and Krenner H J 2013 Acoustically regulated carrier injection into a single optically active quantum dot *Phys. Rev.* B **88** 085307

[13] Buyukkose S, Hernandez-Minguez A, Vratzov B, Somaschini C, Geelhaar L, Riechert H, Van der Wiel W G and Santos P V 2014 High-frequency acoustic charge transport in GaAs nanowires *Nanotechnology* **25** 135204

[14] Graton O, Poulin-Vittrant G, Hue L P T H and Lethiecq M 2013 Strategy of modelling and simulation of electromechanical conversion in ZnO nanowires *Adv. Appl. Ceram.* **112** 85–90

[15] Yin K, Lin H Y, Cai Q, Zhao Y, Lee S T, Hu F and Shao M W 2013 Silicon nanowires nanogenerator based on the piezoelectricity of alpha-quartz *Nanoscale* **5** 12330–4

[16] Hiralal P, Unalan H E and Amaratunga G A 2012 Nanowires for energy generation *Nanotechnology* **23** 194002

[17] Kumar B and Kim S W 2012 Energy harvesting based on semiconducting piezoelectric ZnO nanostructures *Nano Energy* **1** 342–55

[18] Liao Q, Zhang Z, Zhang X, Mohr M, Zhang Y and Fecht H J 2014 Flexible piezoelectric nanogenerators based on a fiber/ZnO nanowires/paper hybrid structure for energy harvesting *Nano Res.* **7** 917–28

[19] Voss T, Bekeny C, Wischmeier L, Gafsi H, Börner S, Schade W, Mofor A C, Bakin A and Waag A 2006 Influence of exciton–phonon coupling on the energy position of the near-band-edge photoluminescence of ZnO nanowires *Appl. Phys. Lett.* **89** 182107

[20] Majidi C, Haataja M and Srolovitz D J 2010 Analysis and design principles for shear-mode piezoelectric energy harvesting with ZnO nanoribbons *Smart Mater. Struct.* **19** 055027

[21] Lu W and Lieber C M 2006 Semiconductor nanowires *J. Phys. D: Appl. Phys.* **39** R387–406

[22] Wauer J and Suherman S 1997 Thickness vibrations of a piezo-semiconducting plate layer *Int. J. Eng. Sci.* **35** 1387–404

[23] Yang J S, Zhou H G, Hu Y T and Jiang Q 2005 Performance of a piezoelectric harvester in thickness-stretch mode of a plate *IEEE Trans. Ultrason. Ferroelectr. Freq. Control* **52** 1872–6

[24] Qin L F, Chen Q M, Cheng H B, Chen Q, Li J F and Wang Q M 2011 Viscosity sensor using ZnO and AlN thin film bulk acoustic resonators with tilted polar c-axis orientations *J. Appl. Phys.* **110** 094511

[25] Navon D H 1986 *Semiconductor Microdevices and Materials* (New York: CBS College Publishing)

[26] Liu J, Fei P, Song J H, Wang X D, Lao C S, Tummala R and Wang Z L 2008 Carrier density and Schottky barrier on the performance of dc nanogenerator *Nano Lett.* **8** 328–32

[27] Wang X B, Song J H, Zhang F, He C Y, Hu Z and Wang Z L 2010 Electricity generation based on one-dimensional group-III nitride nanomaterials *Adv. Mater.* **22** 2155–8